Crosstalk Noise Suppression Between Single and Differential Transmission Lines Using Spoof Surface Plasmon Polaritons

Meini Wang, *Graduate Student Member, IEEE*, Min Tang, *Member, IEEE*, Hao Chi Zhang, *Member, IEEE*, Le Peng Zhang, Tie Jun Cui, *Fellow, IEEE*, and Junfa Mao, *Fellow, IEEE*

***Abstract*— Crosstalk noise suppression is a crux in the high-speed integrated circuit design, which requires weak-coupling between transmission lines (TLs) over a wide band. To overcome the difficulty, this article presents a novel method to suppress the broadband crosstalk noise between a single TL and the differential pair based on spoof surface plasmon polaritons (SPPs). Due to the subwavelength feature of spoof SPP TLs, a natural mode mismatching between the spoof SPP TL and conventional microstrip (MS) brings a broadband suppression of near-field coupling. In order to verify the crosstalk suppression effect, four different kinds of prototypes are discussed and compared. The simulated and measured results in the frequency domain and time domain demonstrate that the proposed scheme achieves more than 83% far-end noise peak suppression than the traditional MS technology by replacing the single MS TL to the spoof SPP TL. Accordingly, the time-domain crosstalk noise is significantly suppressed without any extra costs, demonstrating its potential applications in ultracompact high-speed integrated circuits.**

***Index Terms*— Common-mode noise (CMN), crosstalk noise suppression, differential lines, differential-mode noise (DMN), spoof surface plasmon polaritons (SPPs).**

I. Introduction

With the increase in layout density and working frequency in high-speed circuits, the coupling between parallel transmission lines (TLs) that may induce serious signal integrity (SI) and electromagnetic compatibility (EMC) problems has become a severe challenge [1]. Due to its natural advantage in suppressing electromagnetic interference (EMI), differential microstrip (MS) lines are introduced in the design of high-speed circuits to alleviate this problem [2]. However, for the high-speed transmission of broadband short-pulse signals, the crosstalk noise in the differential lines caused by the neighboring channels is still a headache to designers [3]–[5]. Therefore, it is necessary to propose an effective method to suppress the crosstalk noise between single and differential TLs in high-speed communication systems.

The spoof surface plasmon polariton (SPP) is a kind of novel transmission mode of which the electromagnetic waves propagate parallel to the interface between the metal and the dielectric substrate but decay exponentially in the vertical direction at optical frequencies [6]. It provides a new solution to reduce crosstalk because of the excellent electromagnetic field binding ability and, thus, can be widely used in integrity optical circuits [7], [8]. However, the SPP mode cannot be supported in the microwave and terahertz regimes since the metal exhibits perfect electric conductor (PEC) properties rather than negative permittivity. To break this challenge, a periodic structured surface named spoof SPP has been proposed recently [9], [10]. It can perfectly imitate the propagation characteristics of natural SPPs and also has many advantages, such as strong field confinement, field enhancement, controllable cutoff frequency, and low transmission loss, which can be utilized to build novel TLs [11]–[16]. For example, since the electromagnetic field is highly localized on the surface between the metal and the dielectric substrate, combining with the mode mismatching between the spoof SPP TLs and conventional MS lines, spoof SPPs have been used in the differential interconnect circuits to reduce coupling [17]–[19]. However, the discussion on crosstalk noise suppression in the time domain, which is beneficial to high-speed signal transmission in practical communication systems, has seldom been referred to yet.

In this article, an effective method for broadband crosstalk noise suppression based on spoof SPP TLs is proposed. Several typical cases on the coupling between single and differential TLs are simulated and measured to verify its performance. First, the dispersive characteristics of spoof SPPs and the theoretical analysis of the coupling coefficient are presented. Then, the property of crosstalk noise suppression between aggressive single TL and differential pair using SPP structures is investigated. The numerical simulation and experiment are provided to demonstrate the suppression of crosstalk noise over large bandwidths between single and differential TLs. Finally, some beneficial conclusions are given.

Manuscript received January 12, 2020; revised April 20, 2020 and June 3, 2020; accepted June 20, 2020. Date of publication June 24, 2020; date of current version August 14, 2020. This work was supported in part by the National Natural Science Foundation of China under Grant 61674105, Grant 61831016, and Grant 61831006, and in part by the Guangdong Provincial Key-Field Research Program under Grant 2018B010115001. Recommended for publication by Associate Editor X. Gu upon evaluation of reviewers' comments. *(Corresponding authors: Min Tang; Hao Chi Zhang.)*

Meini Wang, Min Tang, and Junfa Mao are with the Key Laboratory of Ministry of Education of China for Research of Design and Electromagnetic Compatibility of High Speed Electronic Systems, Shanghai Jiao Tong University, Shanghai 200240, China (e-mail: tm222@sjtu.edu.cn).

Hao Chi Zhang, Le Peng Zhang, and Tie Jun Cui are with the State Key Laboratory of Millimeter Waves, Southeast University, Nanjing 210096, China, and also with the Synergetic Innovation Center of Wireless Communication Technology, Southeast University, Nanjing 210096, China.

Color versions of one or more of the figures in this article are available online at http://ieeexplore.ieee.org.

Digital Object Identifier 10.1109/TCPMT.2020.3004593

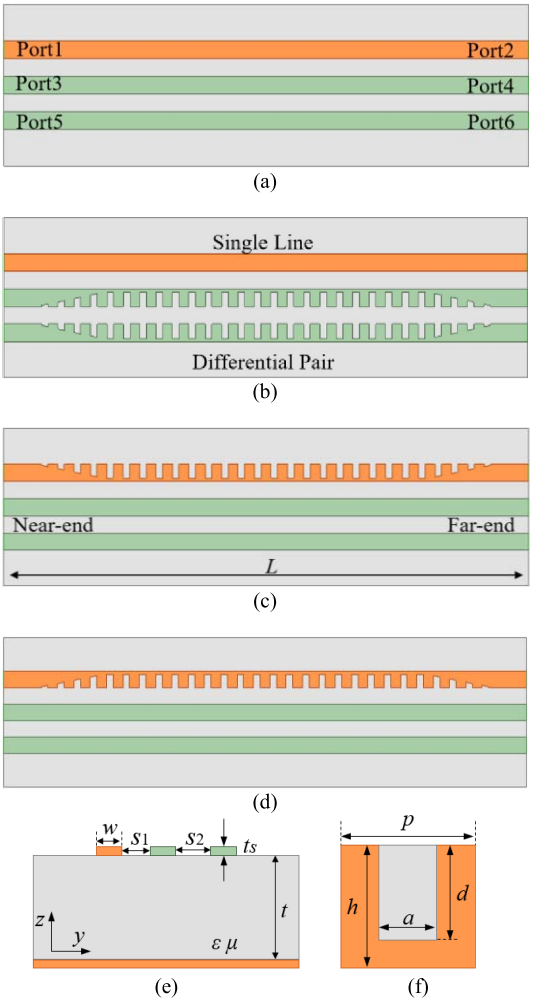

Fig. 1. (a) Differential MS lines coupled with the MS line (Case 1). (b) Differential SPP lines coupled with MS line (Case 2). (c) Differential MS lines coupled with spoof SPP line (Case 3). (d) Differential MS lines coupled with spoof SPP line (Case 4). (e) Cross-sectional view of the coupled section. (f) Unit structure of the spoof SPP TL.

II. Theoretical Analysis

A. Structure of Coupled TLs

In high-speed circuits, due to the demand for miniaturization and integration, high-density wiring has become an inevitable trend; thus, the crosstalk problem caused by it has attracted increasing attention [20]. To explore the method of crosstalk noise suppression, we study four typical coupling cases consisting of an aggressive single line and adjacent differential lines, as shown in Fig. 1.

In Fig. 1(a), both the aggressive single line and coupled differential pair are conventional MS TLs. For comparison, the differential lines are chosen to be SPP TLs in the second case, as shown in Fig. 1(b). The coupling between single SPP TL and MS differential pair is depicted in Fig. 1(c). The case of single SPP TL with the opposite direction of grooves is described in Fig. 1(d). The width $w = 2.44$ mm and thickness $t_s = 0.036$ mm of all TLs are the same, as shown in Fig. 1(e). The total length of all TLs along the x-direction is $L = 80$ mm. Besides, Rogers RT5880 is selected as the dielectric substrate with $\varepsilon_r = 2.2$, loss tangent $\tan\delta = 0.0009$, and thickness $t = 0.787$ mm.

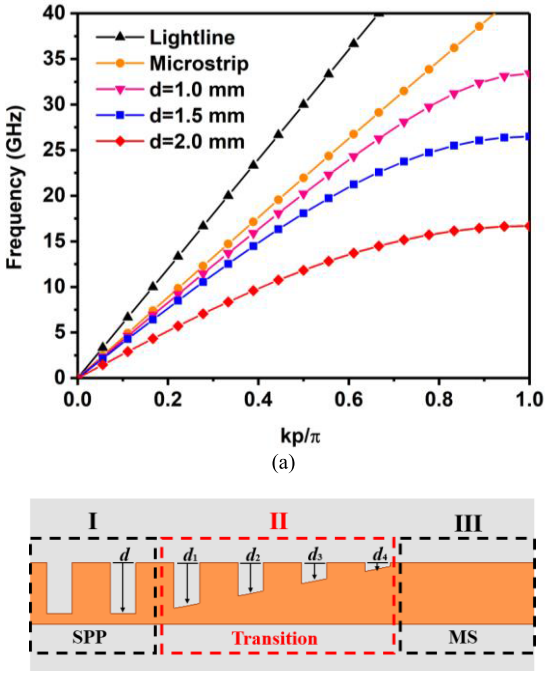

Fig. 2. (a) Dispersive diagrams with different groove depths. (b) Detailed structure for the transition section.

The unit structure of the SPP TLs is shown in Fig. 1(f), in which the period p is 2.5 mm, the width of groove $a = 1$ mm, and the depth of groove $d = 2$ mm. The dispersive curves of spoof SPP TLs with different groove depths in Fig. 2(a) indicates that spoof SPP TLs have larger wavenumber than MS at any fixed frequency. Thus, the electric field energy is more concentrated around the metal guide. Moreover, the strong field confinement of spoof SPP TLs illustrates that it can support the propagation of SPP mode. It is obvious that all dispersive curves of the spoof SPP TLs approach to that of MS with the decrease of depth of grooves, which indicates a smooth transition between the SPP mode and conventional MS mode. Thus, the excitation of the SPP mode can be realized by adding a transition structure with groove depth varying linearly between the spoof SPP TL and the MS line [21], [22]. In this design, the depths at center point of the grooves are set to $d_1 = 1.75$ mm, $d_2 = 1.25$ mm, $d_3 = 0.75$ mm, and $d_4 = 0.25$ mm, respectively, as shown in Fig. 2(b).

B. Theoretical Analysis

To analyze the coupling property of these different cases in theory, the coupling coefficients are evaluated in this part. According to coupled-mode theory and the reciprocity of system [23], the coupling of parallel lossless TLs can be written as

$$\frac{dA_1}{dx} = i\beta_1 A_1 + ik_{12}A_2 + ik_{13}A_3 \quad (1)$$

$$\frac{dA_2}{dx} = ik_{12}A_1 + i\beta_2 A_2 + ik_{23}A_3 \quad (2)$$

$$\frac{dA_3}{dx} = ik_{13}A_1 + ik_{23}A_2 + i\beta_3 A_3 \quad (3)$$

where A_j $(j = 1, 2, 3)$ expresses the modal amplitude, β_j is the mode phase constant of TL j, and k_{ij} is the coupling coefficient.

First, the coupling coefficients in different cases are investigated. Between two MS TLs, it can be obtained as

$$k_{ij}^{\mathrm{MS}} = \frac{\omega\varepsilon_0}{4}\int\int_{-\infty}^{\infty}\left(n^2 - n_0^2\right)\vec{E}_{it}^{*}\cdot\vec{E}_{jt}dydz \tag{4}$$

where $\vec{E}_{jt}$ is transverse electric field distribution of line j, n is the refractive index of the neighboring medium, n_0 is the refractive index of TLs, ω is the angular frequency, and ε_0 is the vacuum dielectric constant.

By contrast, the SPP TL does not satisfy the weak derivative approximation condition because, in the optical sense, its core refractive index and cladding refractive index are quite different [24]. As a result, the longitudinal electric field component $\vec{E}_{jx}$ needs to be considered, and the coupling coefficient between two SPP TLs can be expressed as

$$k_{ij}^{\mathrm{SPP}} = \frac{\omega\varepsilon_0}{4} \times \int\int_{-\infty}^{\infty}\left(n^2 - n_0^2\right)\left[\vec{E}_{it}^{*}\cdot\vec{E}_{jt} + \left(\frac{n_0^2}{n^2}\right)\vec{E}_{ix}^{*}\cdot\vec{E}_{jx}\right]dydz. \tag{5}$$

Note that in the condition of coupling between MS and SPP, (5) can be simplified into (4).

As indicated in (4) and (5), the coupling coefficient is only decided by the electric field energy of the overlapping region between coupled TLs when the working frequency and the surrounding environment are determined. Since the electromagnetic field is strongly enhanced around the metal groove, the energy can hardly be coupled to others. Therefore, the overlap of electric field energy in coupled structures with the SPP TLs is much smaller than that of the traditional MS TLs, which is beneficial to crosstalk noise suppression.

To further investigate the coupling property, the coupling power ratios (CPRs) of TLs are studied for the abovementioned different cases. In Case 1, the coefficient matrix B_1 of differential equations (1)–(3) can be written as

$$B_1 = i\begin{pmatrix}\beta_m & k_{12} & 0\\ k_{12} & \beta_m & k_{23}\\ 0 & k_{23} & \beta_m\end{pmatrix} \tag{6}$$

where β_m is the phase constant of the MS line. Note that due to the little contribution of k_{13} compared with others, it is ignored in the derivation.

The analytical solutions of equations are indicated by

$$A_1 = \frac{e^{i\beta_m x}}{k_{12}^2 + k_{23}^2}\left(k_{23}^2 + k_{12}^2\cos\left(\sqrt{k_{12}^2 + k_{23}^2}x\right)\right) \tag{7}$$

$$A_2 = \frac{ie^{i\beta_m x}}{\sqrt{k_{12}^2 + k_{23}^2}}k_{12}\sin\left(\sqrt{k_{12}^2 + k_{23}^2}x\right) \tag{8}$$

$$A_3 = \frac{e^{i\beta_m x}}{k_{12}^2 + k_{23}^2}k_{12}k_{23}\left(1 + \cos\left(\sqrt{k_{12}^2 + k_{23}^2}x\right)\right). \tag{9}$$

Hence, the CPR of C_{14} at port 4 can be expressed as

$$C_{14} = \frac{|A_2(L)|^2}{|A_1(0)|^2} = \frac{k_{12}^2}{k_{12}^2 + k_{23}^2}\sin^2\left(\sqrt{k_{12}^2 + k_{23}^2}L\right). \tag{10}$$

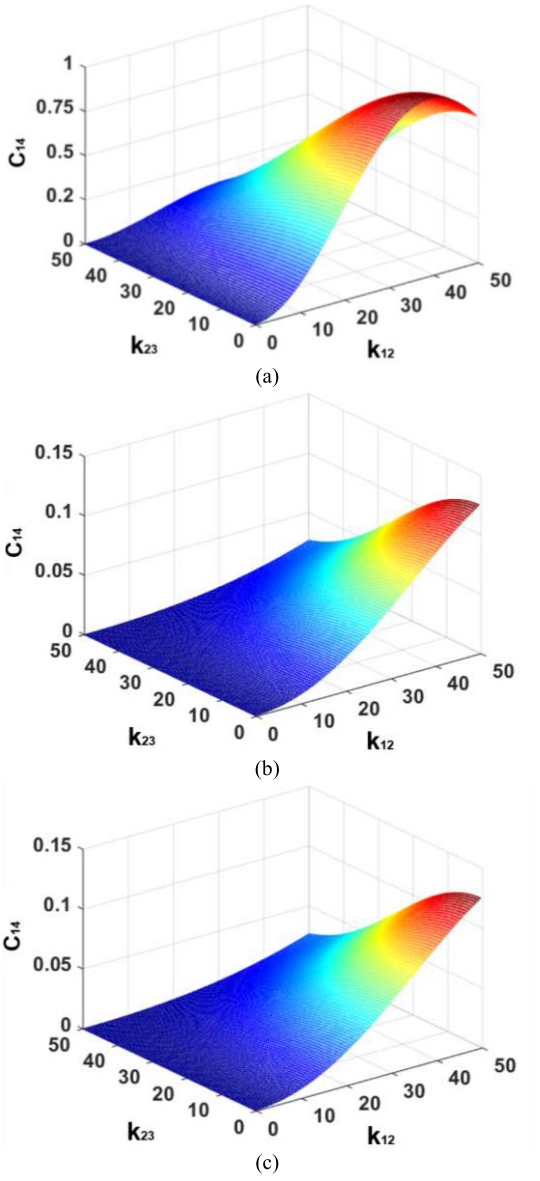

Fig. 3. Variation of C_{14} with k_{12} and k_{23}. (a) Case 1. (b) Case 2. (c) Cases 3 and 4.

Similarly, the coefficient matrices in Cases 2–4 can be, respectively, written as

$$B_2 = i\begin{pmatrix}\beta_m & k_{12} & 0\\ k_{12} & \beta_s & k_{23}\\ 0 & k_{23} & \beta_s\end{pmatrix} \tag{11}$$

and

$$B_3 = B_4 = i\begin{pmatrix}\beta_s & k_{12} & 0\\ k_{12} & \beta_m & k_{23}\\ 0 & k_{23} & \beta_m\end{pmatrix} \tag{12}$$

where β_s is the phase constant of the spoof SPP line. Referring to the derivation process of Case 1, the corresponding CPR as the function of k_{12} and k_{23} can be obtained in turn.

For illustration, we assume that the length of TLs in Fig. 1 is $L = 40$ mm, and the operating frequency is 10 GHz. The corresponding relationship between C_{14} and the coupling coefficient k_{ij} is depicted in Fig. 3.

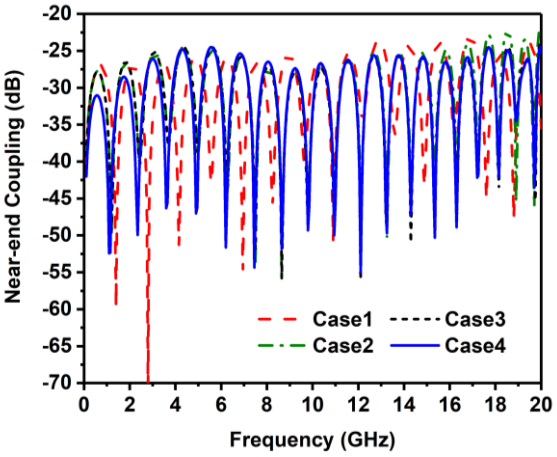

(a)

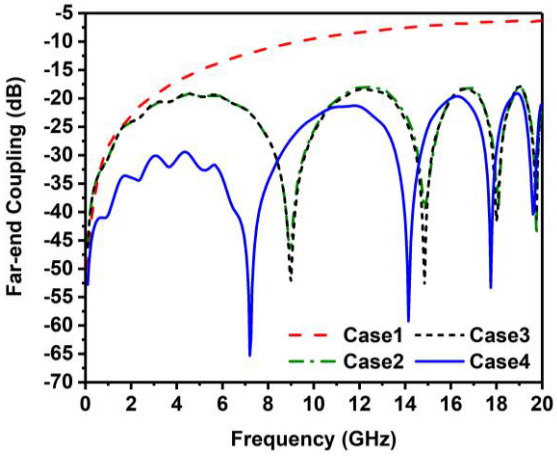

(b)

Fig. 4. Simulated S-parameters of coupled structures. (a) Near-end coupling S_{31}. (b) Far-end coupling S_{41}. The port naming is the same as that in Fig. 1(a).

It is obvious that the CPRs in all cases are positively correlated with k_{12} and negatively correlated with k_{23}. If k_{12} and k_{23} are fixed at certain values, the CPR of Case 1 is much larger than the others, which verifies the coupling suppression capability of the spoof SPP TL. Furthermore, since Case 4 holds the smallest k_{12} and relatively large k_{23} over the four cases, it exhibits the best performance in crosstalk suppression, which will be demonstrated by simulation and measurement in the following.

III. Simulated Results

In order to analyze the coupled crosstalk of four kinds of models in Fig. 1, port 1 of the aggressive single line is excited, and we obtain the S-parameters of the abovementioned structures by full-wave electromagnetic solver ANSYS HFSS.

To investigate the impact of the aggressive line to the neighboring differential TLs, the near- and far-end coupling properties on the most adjacent line are shown in Fig. 4(a) and (b), respectively. It is seen that the near-end coupling S_{31} of investigated structures is below -20 dB, which indicates that the spoof SPP TLs are similar to conventional MS lines in near-end crosstalk (NEXT) performance.

As for the far-end coupling, however, significant suppression of crosstalk is achieved with the utilization of SPP TLs, as compared in Fig. 4(b). In Case 4, for instance, the far-end coupling keeps lower than -20 dB over a wide bandwidth from 0 to 20 GHz. By contrast, the far-end coupling S_{41} of conventional MS TLs increases with frequency and reaches up to -6.29 dB at 20 GHz, as illustrated in Case 1. Thus, we obtain that, by introducing spoof SPPs, the crosstalk of coupled structures can be reduced drastically.

Furthermore, we also observe that the groove direction of the single SPP TL will affect the coupling performance apparently. According to the comparison between Cases 3 and 4, the structure of single spoof SPP TL with the groove direction toward the differential TLs has better suppression performance on the far-end coupling since the electric field energy is localized on the side of the metal groove rather than the other. Thus, the structure in Case 4 holds better performance in crosstalk noise suppression.

Based on the results obtained in the frequency domain, the time-domain noise suppression property of the abovementioned structures is investigated by ADS. A typical high-speed pulse signal with an amplitude of 1 V, rise/fall time of 50 ps, and width 0.7 ns, is excited at port 1 of the aggressive line. Then, we obtain the NEXT and far-end crosstalk (FEXT) of the differential lines with matched loads. The components of differential-mode noise (DMN) and common-mode noise (CMN) are acquired by the data processing, and they are discussed, respectively.

In general, the NEXT noise appears as a wide pulse with low amplitude in time, while the FEXT noise appears as a narrow pulse with a high amplitude. The results of NEXT and FEXT noises for different cases are shown in Fig. 5.

From Fig. 5(a) and (b), we observe that both the CMN and DMN at the near end of differential TLs are reduced by spoof SPP TLs in Case 4. However, the improvement in Cases 2 and 3 is not apparent although the spoof SPP technique is utilized. These phenomena are in accordance to the frequency-domain results in Fig. 4(a).

However, as for the crosstalk noise at the far end, the results are quite different, as shown in Fig. 5(c) and (d). It is obvious that both the CMN and DMN at the far end of differential TLs can be effectively suppressed by using spoof SPP TLs. Especially in Case 4, the relative peak values of CMN and DMN are reduced by 84% and 88%, respectively, compared with conventional MS lines, which is rather beneficial to SI performance in the high-density integrated circuits.

Since the gap between lines is a crucial parameter for coupling performance, we consider the far-end effect of spoof SPP coupled structures comparing with MS lines on crosstalk noise suppression in cases of different gaps. Taking the Cases 1, 3, and 4 as examples, the peaks of crosstalk noise with different gaps between the single line and differential pair are listed in Table I. We observe that the relative peak values of CMN or DMN decrease by 38%–60% in Case 3 and 70%–90% in Case 4 comparing with Case 1, which indicates that the FEXT noise can be effectively suppressed by spoof SPPs for both strong- and weak-coupling conditions.

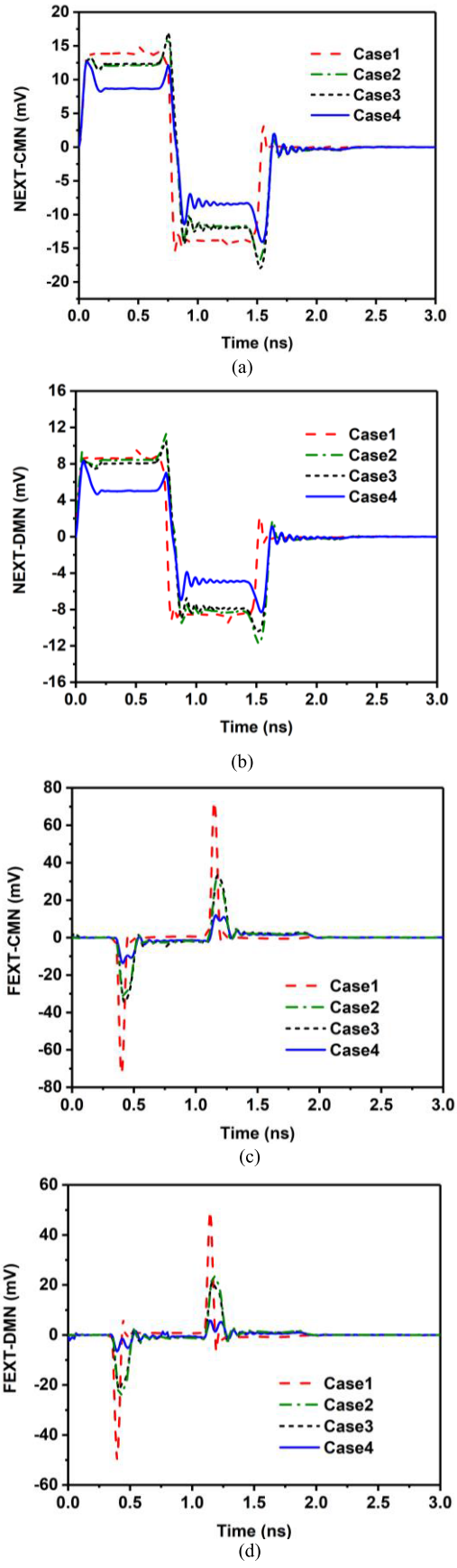

Fig. 5. Simulated results of (a) CMN and (b) DMN due to NEXT and (c) CMN and (d) DMN due to FEXT.

TABLE I
CROSSTALK NOISE PEAKS WITH DIFFERENT GAPS

$s1$	CMN/DMN (mV)			ΔCMN/DMN (%)	
	Case1	Case3	Case4	Δ1	Δ2
0.5w	110/78	58/40	11/11	47/38	90/86
w	73/50	33/21	**12/6**	40/48	84/88
1.5w	48/30	21/12	10/5	56/60	79/83
2w	32/16	**14/7**	8/4	56/56	75/75
2.5w	22/10	10/5	6/3	55/50	72/70
3w	**17/7**	8/4	5/2	53/43	70/71

$s1$ is the gap between the single line and the differential pair. ΔCMN/DMN is the relative peak reduction of common mode and differential mode noise for Case3 (Δ1) and Case4 (Δ2) comparing with Case1.

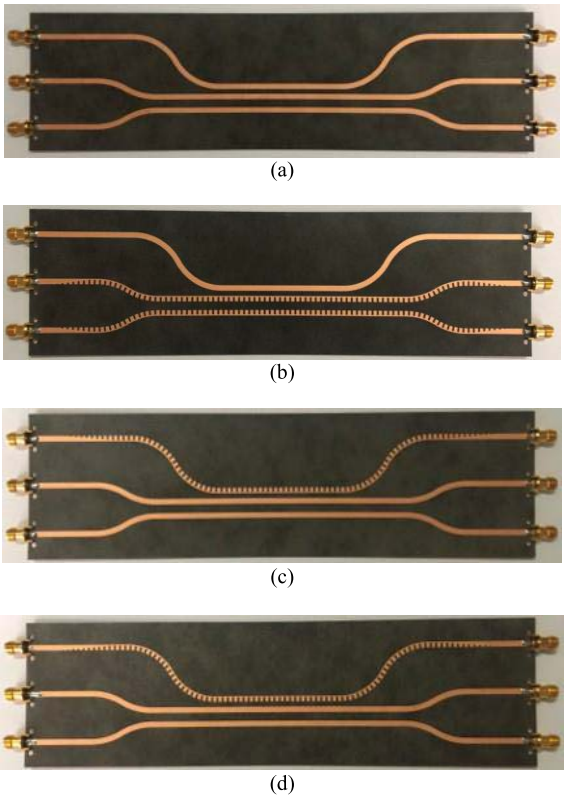

Fig. 6. Experimental samples of coupled TLs. (a) Case 1. (b) Case 2. (c) Case 3. (d) Case 4.

In addition, for the traditional MS lines, three times trace width is commonly used in practice for wire spacing, where the crosstalk can be safely ignored. As illustrated by the results with bold font in Table I, when $s_1 = 3w$ (Case 1), the peak values of CMN and DMN are 17 and 7 mV, respectively. In the cases with spoof SPP lines (Cases 3 and 4), the wire spacing can be, respectively, reduced to $2w$ and w under the premise of a similar noise peak level. It is obvious that the introduction of a spoof SPP structure is rather beneficial for saving wiring space and reducing crosstalk.

IV. EXPERIMENTAL VERIFICATION

To demonstrate the crosstalk characteristics of the above-mentioned coupled structures, four samples are fabricated, as shown in Fig. 6(a)–(d). Considering the actual measurement

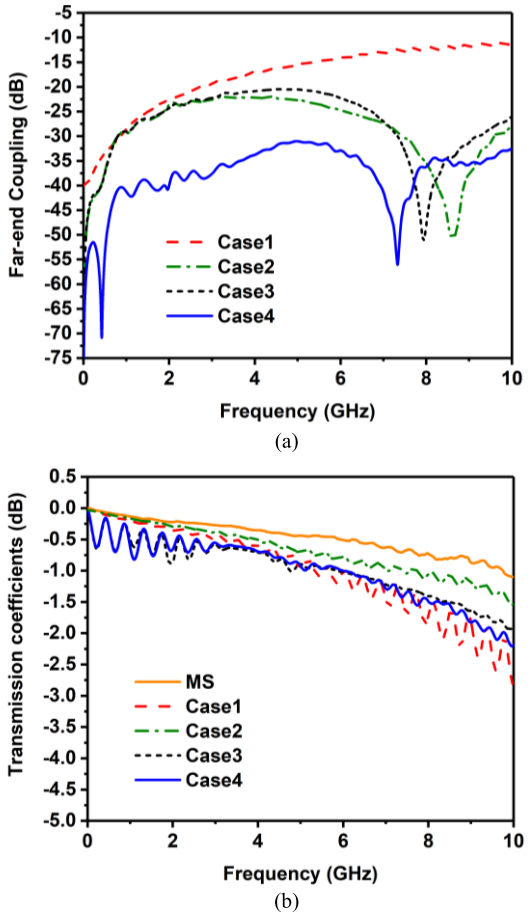

Fig. 7. Comparison of measured results. (a) Far-end coupling coefficient S_{41}. (b) Transmission coefficient S_{21}.

with SMA connectors, TLs are designed in a curved shape. The coupling length ($L1$) of the middle parallel part is fixed as 60 mm, while the total length (L) along the x-direction is 240 mm in all cases. The gaps $s1$ and $s2$ are 2.44 and 4 mm, respectively. In our design, the characteristic impedance of a single MS line is 50 Ω, while the differential impedance of coupled MS lines is 96 Ω. The signal is imposed on port 1, and the S-parameters are measured at all six ports by vector network analyzer (VNA). The far-end coupling S_{41} represents the crosstalk between the differential pair and a single line. As shown in Fig. 7(a), the crosstalk is suppressed significantly with the utilization of SPP TLs. Among them, Case 4 holds the best performance, where the far-end coupling keeps lower than −30 dB over a wide bandwidth. The phenomenon is consistent with the simulated results in Section III.

Besides the crosstalk, the transmission loss of aggressive TL is also important. The measured transmission coefficients in different cases are compared in Fig. 7(b), where the performance of a single MS line is provided for benchmarking. The insertion loss of TL comes from several aspects, such as the transition structures, bended structures, coupling from adjacent lines, conductor loss, dielectric loss, as well as the impact of SMA connectors. From the measured results in Fig. 7(b), it is obtained that the transmission performance of the MS line in Case 2 is the best since no transition structures are utilized, and the coupling between MS and SPP TLs is

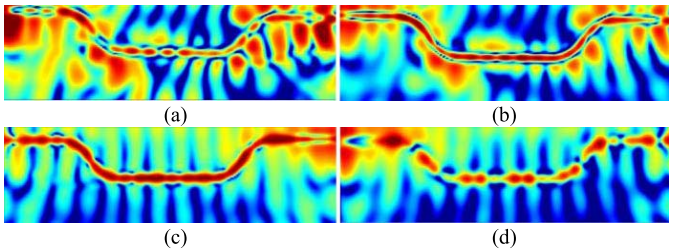

Fig. 8. Measured electric field distribution at 10 GHz in different cases. (a) Case 1. (b) Case 2. (c) Case 3. (d) Case 4.

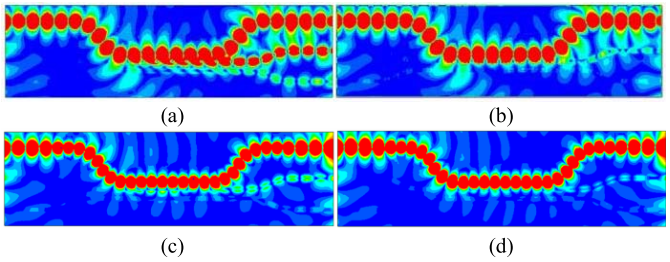

Fig. 9. Simulated electric field distribution at 10 GHz in different cases. (a) Case 1. (b) Case 2. (c) Case 3. (d) Case 4.

weak. Thus, the impact of impedance discontinuity in Case 2 is the smallest. We also observe that Cases 3 and 4 have similar transmission performance to Case 1, which indicates that introducing spoof SPPs in the aggressive TL will not deteriorate the transmission loss apparently.

Furthermore, to investigate the near-field characteristics of the coupled models, the electric field energy on a plane 1 mm above the TLs is measured. We set up the experimental platform in a microwave anechoic chamber where the detecting probe configured by a monopole antenna that is automatically controlled by a stepper motor.

The measured results of electric field distribution are obtained in Fig. 8(a)–(d). In Fig. 8(a) and (b), we clearly observe that a large part of electric field energy diffuses from the single MS line to the adjacent differential lines. Especially, the coupling effect at the far end of TLs is obvious.

Much better results are obtained when the SPP is introduced into the aggressive single line, as shown in Fig. 8(c) and (d). It is seen that almost all the electric field energy is concentrated around the single line, which verifies that the subwavelength periodically corrugated metal lines with strong electromagnetic field confinement can suppress the crosstalk noise effectively. The corresponding simulated results of the same plane are shown in Fig. 9, which are in accordance with the experiment.

In order to provide more intuitive results, the time-domain properties of the coupled structures are investigated based on the measured S-parameters. Assume that the excitation signal is imposed on port 1 of the single aggressive line; the voltage responses at the far end of the line in different cases are compared in Fig. 10. Due to the slow wave effects, the time delay values in Cases 3 and 4 are larger than those in Cases 1 and 2. The ringing phenomena in Cases 3 and 4 are attributed to the transition structures of SPP TLs.

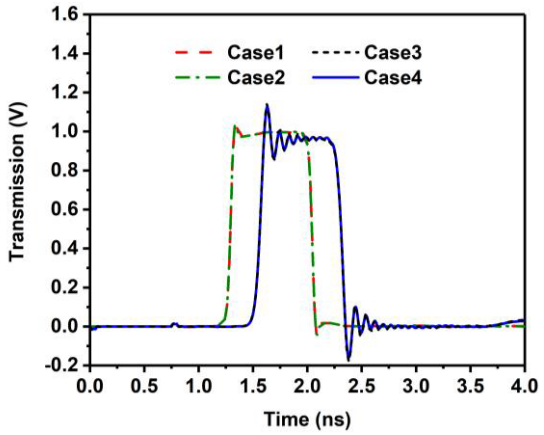

Fig. 10. Comparison of voltage responses at the far end of the aggressive line.

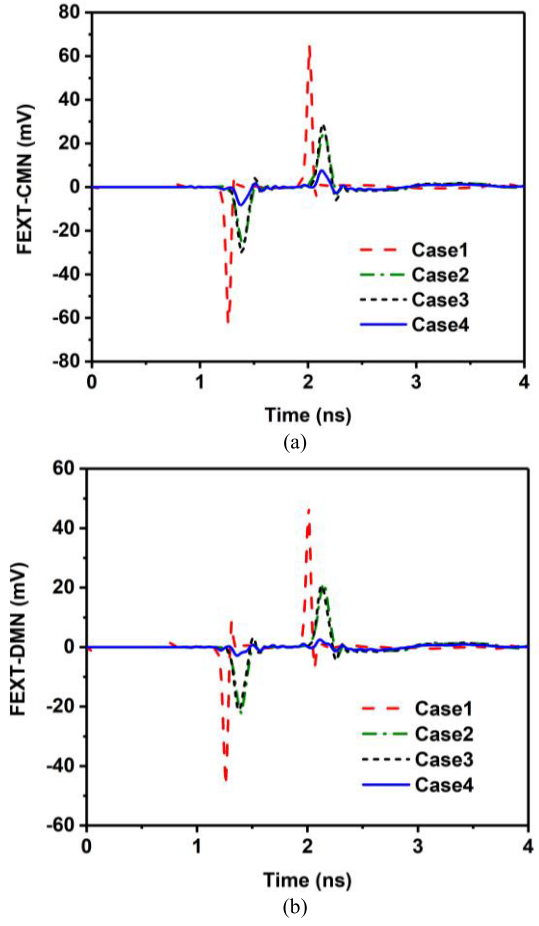

Fig. 11. Results of (a) CMN and (b) DMN at the far end of different structures.

As for the crosstalk issue, comparing with the far-end coupling, the near-end crosstalk noise is relatively small; thus, we will focus on the noise suppression effect at the far end. It is obvious that both the CMN and DMN at the far end of differential lines in Fig. 11 are suppressed owing to the utilization of spoof SPP TLs. The maximum CMN and DMN of the conventional MS lines are 67.5 and 44.5 mV, as listed in Table II, respectively. They are reduced to 7.5 and 2.5 mV, respectively, in Case 4. Thus, we obtain that the spoof SPP TL provides an effective way for crosstalk suppression in high-speed circuits.

TABLE II
FEXT PEAK IN DIFFERENT STRUCTURES

FEXT	Case1	Case2	Case3	Case4	Δ2
CMN (mV)	67.5	25.5	29.5	7.5	88.9%
DMN (mV)	44.5	21.5	20.5	2.5	94.4%

Δ2 is the relative peak reduction of common mode and differential mode noise for Case4 comparing with Case1.

V. CONCLUSION

In this article, the method for crosstalk noise suppression between a single signal line and adjacent differential pair is investigated. Due to the strong field confinement ability and property of mode mismatching with conventional MS lines, the spoof SPP TLs contribute significantly to the suppression of crosstalk noise. The simulation and experiment in both time and frequency domains illustrate that spoof SPP TLs can effectively reduce crosstalk between parallel TLs in high-density integrated circuits, which is beneficial for EMC in high-speed communication systems.

REFERENCES

[1] T.-L. Wu, F. Buesink, and F. Canavero, "Overview of signal integrity and EMC design technologies on PCB: Fundamentals and latest progress," *IEEE Trans. Electromagn. Compat.*, vol. 55, no. 4, pp. 624–638, Aug. 2013.
[2] P. E. Fornberg, M. Kanda, C. Lasek, M. Piket-May, and S. H. Hall, "The impact of a nonideal return path on differential signal integrity," *IEEE Trans. Electromagn. Compat.*, vol. 44, no. 1, pp. 11–15, Feb. 2002.
[3] J. Martel, A. Fernandez-Prieto, A. Lujambio, F. Medina, F. Mesa, and R. R. Boix, "Differential lines for common-mode suppression based in hybrid microstrip/CPW technology," *IEEE Microw. Wireless Compon. Lett.*, vol. 27, no. 1, pp. 13–15, Jan. 2017.
[4] S. Lee, J. Lim, S. Oh, Y. Kim, D. Oh, and J. Lee, "Differential-to-common-mode conversion suppression using mushroom structure on bent differential transmission lines," *IEEE Trans. Compon., Packag., Manuf. Technol.*, vol. 9, no. 4, pp. 702–711, Apr. 2019.
[5] C.-C. Yeh, K.-C. Chen, and C.-L. Wang, "Common-mode noise suppression of differential serpentine delay line using timing-offset differential signal," *IEEE Trans. Electromagn. Compat.*, vol. 57, no. 6, pp. 1457–1465, Dec. 2015.
[6] S. A. Maier, *Plasmonics: Fundamentals and Applications*. New York, NY, USA: Springer, 2007.
[7] L. Liu, Z. Han, and S. He, "Novel surface plasmon waveguide for high integration," *Opt. Express*, vol. 13, no. 17, pp. 6645–6650, Oct. 2018.
[8] J. J. Wu *et al.*, "Differential microstrip lines with reduced crosstalk and common mode effect based on spoof surface plasmon polaritons," *Opt. Express*, vol. 22, no. 22, pp. 26777–26787, Nov. 2014.
[9] J. B. Pendry, "Mimicking surface plasmons with structured surfaces," *Science*, vol. 305, no. 5685, pp. 847–848, Aug. 2004.
[10] A. P. Hibbins, "Experimental verification of designer surface plasmons," *Science*, vol. 308, no. 5722, pp. 670–672, Apr. 2005.
[11] T. J. Cui, "Microwave metamaterials," *Nat. Sci. Rev.*, vol. 5, no. 2, pp. 134–136, 2018.
[12] L. P. Zhang, H. C. Zhang, Z. Gao, and T. J. Cui, "Measurement method of dispersion curves for spoof surface plasmon polaritons," *IEEE Trans. Antennas Propag.*, vol. 67, no. 7, pp. 4920–4923, Jul. 2019.
[13] H. C. Zhang *et al.*, "Dispersion analysis of deep-subwavelength-decorated metallic surface using field-network joint solution," *IEEE Trans. Antennas Propag.*, vol. 66, no. 6, pp. 2923–2933, Jun. 2018.
[14] L. Liu *et al.*, "Multi-channel composite spoof surface plasmon polaritons propagating along periodically corrugated metallic thin films," *J. Appl. Phys.*, vol. 116, no. 1, Jul. 2014, Art. no. 013501.

[15] H. C. Zhang, Q. Zhang, J. F. Liu, W. Tang, Y. Fan, and T. J. Cui, "Smaller-loss planar SPP transmission line than conventional microstrip in microwave frequencies," *Sci. Rep.*, vol. 6, no. 1, Mar. 2016, Art. no. 023396.
[16] H. C. Zhang, S. Liu, X. Shen, L. H. Chen, L. Li, and T. J. Cui, "Broadband amplification of spoof surface plasmon polaritons at microwave frequencies," *Laser Photon. Rev.*, vol. 9, no. 1, pp. 83–90, Nov. 2014.
[17] S. Zhao, H. C. Zhang, L. Liu, J. Zhao, and C. Yang, "A novel low-crosstalk driveline based on spoof surface plasmon polaritons," *IEEE Access*, vol. 7, pp. 30702–30707, 2019.
[18] H. C. Zhang, T. J. Cui, Q. Zhang, Y. Fan, and X. Fu, "Breaking the challenge of signal integrity using time-domain spoof surface plasmon polaritons," *ACS Photon.*, vol. 2, no. 9, pp. 1333–1340, Aug. 2015.
[19] X. Gao *et al.*, "Crosstalk suppression based on mode mismatch between spoof SPP transmission line and microstrip," *IEEE Trans. Compon., Packag., Manuf. Technol.*, vol. 9, no. 11, pp. 2267–2275, Nov. 2019.
[20] L. H. K. Duong *et al.*, "Crosstalk noise reduction through adaptive power control in inter/intra-chip optical networks," *IEEE Trans. Comput.-Aided Design Integr. Circuits Syst.*, vol. 38, no. 1, pp. 43–56, Jan. 2019.
[21] W. Zhang, G. Zhu, L. Sun, and F. Lin, "Trapping of surface plasmon wave through gradient corrugated strip with underlayer ground and manipulating its propagation," *Appl. Phys. Lett.*, vol. 106, no. 2, Jan. 2015, Art. no. 021104.
[22] H. C. Zhang *et al.*, "Active digital spoof plasmonics," *Nat. Sci. Rev.*, vol. 7, no. 2, pp. 261–269, Feb. 2020.
[23] A. Yariv, "Coupled-mode theory for guided-wave optics," *IEEE J. Quantum Electron.*, vol. 9, no. 9, pp. 919–933, Sep. 1973.
[24] A. Ma, Y. Li, and X. Zhang, "Coupled mode theory for surface plasmon polariton waveguides," *Plasmonics*, vol. 8, no. 2, pp. 769–777, Jun. 2013.

Meini Wang (Graduate Student Member, IEEE) received the B.S. degree in electronic information science and technology from Jilin University, Changchun, China, in 2014. She is currently pursuing the Ph.D. degree in electronic science and technology with Shanghai Jiao Tong University, Shanghai, China.

Her current research interests include microwave theory and techniques, surface plasmon, and antennas.

Min Tang (Member, IEEE) was born in 1980. He received the B.S. degree in electronic engineering from Northwestern Polytechnical University, Xi'an, China, in 2001, the M.S. degree in electrical engineering from Xi'an Jiaotong University, Xi'an, in 2004, and the Ph.D. degree in electronic engineering from Shanghai Jiao Tong University, Shanghai, China, in 2007.

Since 2007, he has been a Faculty Member with Shanghai Jiao Tong University, where he is currently an Associate Professor with the Department of Electronic Engineering. He was a Post-Doctoral Research Fellow with The University of Hong Kong, Hong Kong, from 2010 to 2012. His research interests include signal and power integrity of high-speed circuits, and multiscale and multiphysics modeling of integrated systems.

Hao Chi Zhang (Member, IEEE) received the B.Eng. degree in electrical engineering from the University of Electronic Science and Technology of China, Chengdu, China, in 2013. He is currently pursuing the Ph.D. degree in electromagnetic and microwave technology with Southeast University, Nanjing, China.

He is currently a Project Officer with the School of Electrical and Electronic Engineering, Nanyang Technological University, Singapore. He has authored over 30 international refereed journal articles, in highly ranked journals, including *Laser & Photonics Review*, *ACS Photonics*, the IEEE TRANSACTIONS ON ANTENNAS AND PROPAGATION, and *Applied Physics Letters*. His current research interests include microwave and millimeter-wave circuits and antennas technology, surface plasmon, and metamaterials.

Le Peng Zhang received the B.S. degree in electronic information engineering from Xidian University, Xi'an, China, in 2018. He is currently pursuing the Ph.D. degree in electromagnetic and microwave technology with Southeast University, Nanjing, China.

His research interests lie in the areas of microwave and millimeter-wave circuits and antennas technology, surface plasmon, and metamaterials.

Tie Jun Cui (Fellow, IEEE) received the B.Sc., M.Sc., and Ph.D. degrees in electrical engineering from Xidian University, Xi'an, China, in 1987, 1990, and 1993, respectively.

In March 1993, he joined the Department of Electromagnetic Engineering, Xidian University, where he was promoted to an Associate Professor in November 1993. From 1995 to 1997, he was a Research Fellow with the Institut für Höchstfrequenztechnik und Elektronik (IHE), University of Karlsruhe, Karlsruhe, Germany. In July 1997, he joined the Center for Computational Electromagnetics, Department of Electrical and Computer Engineering, University of Illinois at Urbana–Champaign, Champaign, IL, USA, first as a Post-Doctoral Research Associate and then a Research Scientist. In September 2001, he was a Cheung-Kong Professor with the Department of Radio Engineering, Southeast University, Nanjing, China, where he became a Chief Professor in January 2018. He is the first author of the following books: *Metamaterials: Theory, Design, and Applications* (Springer, Nov. 2009) and *Metamaterials: Beyond Crystals, Noncrystals, and Quasicrystals* (CRC Press, March 2016). He has published over 500 peer-reviewed journal articles, which have been cited by more than 24 000 times (H-Factor 78; from Google Scholar) and licensed over 60 patents.

Dr. Cui was awarded a Research Fellowship from the Alexander von Humboldt Foundation, Bonn, Germany, in 1995, and a Cheung Kong Professor under the Cheung Kong Scholar Program by the Ministry of Education, China, in 2001, and received the Young Scientist Award from the International Union of Radio Science in 1999 and the National Science Foundation of China for Distinguished Young Scholars in 2002. He also received the Natural Science Award (First Class) from the Ministry of Education, China, in 2011, and the National Natural Science Awards of China (Second Class) in 2014 and 2018, respectively. His research has been selected as one of the most exciting peer-reviewed optics research "Optics in 2016" by *Optics & Photonics News Magazine* (OSA), 10 Breakthroughs of China Science in 2010, "Best of 2010" in the *New Journal of Physics*, and Research Highlights in a series of journals. His work has been widely reported by Nature News, MIT Technology Review, Scientific American, Discover, New Scientists, and so on.

Junfa Mao (Fellow, IEEE) was born in 1965. He received the B.S. degree in radiation physics from the National University of Defense Technology, Changsha, China, in 1985, the M.S. degree in experimental nuclear physics from the Shanghai Institute of Nuclear Research, Chinese Academy of Sciences, Beijing, China, in 1988, and the Ph.D. degree in electronic engineering from Shanghai Jiao Tong University, Shanghai, China, in 1992.

Since 1992, he has been a Faculty Member with Shanghai Jiao Tong University, where he is currently a Chair Professor and the Vice-President. He was a Visiting Scholar with The Chinese University of Hong Kong, Hong Kong, from 1994 to 1995, and a Post-Doctoral Researcher with the University of California at Berkeley, Berkeley, CA, USA, from 1995 to 1996. He has authored or coauthored more than 500 articles (including more than 130 IEEE journal articles). His research interests include interconnect and package problems of integrated circuits and systems, and analysis and design of microwave components and circuits.